R-117

DAVIDSON LABORATORY

REPORT 1170

STEVENS INSTITUTE
OF TECHNOLOGY
CASTLE POINT STATION
HOBOKEN, NEW JERSEY

HYDROFOIL FLUTTER PHENOMENON AND AIRFOIL FLUTTER THEORY

Volume IV, Finite Aspect Ratio

by

Charles J. Henry

and

M. Raihan Ali

October 1966

DAVIDSON LABORATORY

REPORT 1170

October 1966

HYDROFOIL FLUTTER PHENOMENON AND AIRFOIL FLUTTER THEORY

Volume IV, Finite Aspect Ratio

by

Charles J. Henry

and

M. Raihan Ali

Prepared for the
Bureau of Ships, Department of the Navy
Contract NObs 88365, Task 1719
Project Serial No. SS 600-00

(DL Project 2709/227)

Approved

S. Tsakonas

S. Tsakonas, Chief
Fluid Dynamics Division

ix + 36 pages
4 tables
5 figures

ABSTRACT

Measured decay rates and flutter speeds for two-degree-of-freedom hydrofoil models with finite aspect ratio are compared with those predicted by two-dimensional airfoil theory applied in a stripwise manner. The flutter speed of one of the experimental configurations is also predicted by means of three-dimensional lifting-surface theory. Both theory and experiment indicate that flutter speed increases as aspect ratio is decreased. However, the non-conservative discrepancy found previously between measured and predicted two-degree-of-freedom flutter speeds in two-dimensional flow persists in these three-dimensional results.

KEYWORDS

Hydroelasticity

Flutter

TABLE OF CONTENTS

NOMENCLATURE

A	ratio of spanwise reference length to chordwise reference length
$A,B,C,$	parameters defined in Equation (67)
b_o	reference semichord length
e_o	dimensionless distance from y-axis to rotational axis in units of b_o, positive if the rotational axis is aft
$F_h, F_\alpha, T_h, T_\alpha$	harmonic hydrodynamic derivatives from two-dimensional strip theory
$f_j(x,y)$	j^{th} displacement mode shape
H	hydrofoil planform area
i	$\sqrt{-1}$
$K(x,y;\xi,\eta;\omega)$	kernel function for calculating harmonic response at frequency ω
$K_1(x,y,t;\xi,\eta,\tau)$	kernel function for calçulating indicial response
k	$\omega b_o/U$ = reduced frequency
$L_{11}, L_{12}, L_{21}, L_{22}$	harmonic hydrodynamic derivatives from three-dimensional theory
$L_{\ddot{q}_j}, L_{\dot{q}_j}, M_{\ddot{q}_j}, M_{\dot{q}_j}$	indicial hydrodynamic derivatives
M	total mass of hydrofoil configuration
$M_{j\ell}$	generalized mass

$\Delta p(x,y,t)$	unsteady pressure-loading on hydrofoil
$\bar{p}_j(x,y,\omega)$	harmonic pressure-response function
$p_{NC}(x,y)$	non-circulatory component of indicial pressure response
$p_{QS}(x,y)$	quasi-steady component of indicial pressure response
$p_{US}(x,y,t)$	unsteady component of indicial pressure response
$Q_j(t)$	generalized force in j^{th} degree of freedom
$q_j(t)$	generalized coordinate in j^{th} degree of freedom
r_α	dimensionless radius of gyration of hydrofoil configuration about rotational axis, in semichords
s	spanwise reference length
T	taper ratio (tip chord/root chord)
T(t)	time dependence of hydrofoil motion
t	time
U	forward speed of hydrofoil
U_F	flutter speed
x,y	orthogonal Cartesian coordinate system
x_α	dimensionless distance from rotational axis to center of gravity in semichords, positive if CG is aft
Z(x,y)	space dependence of hydrofoil motion

Λ	midchord sweep angle
μ	density ratio
μ_{CR}	critical density ratio
ρ	fluid density
Ω	dimensionless natural frequency in rotational degree of freedom
ω	response frequency
ω_j	uncoupled natural frequency in j^{th} mode

INTRODUCTION

In two earlier hydroelastic studies at the Davidson Laboratory,[1,2] measured response characteristics and flutter speeds of several two-degree-of-freedom hydrofoil models in two-dimensional flow were compared with corresponding results predicted by two-dimensional airfoil theory. These models were tested over a range of density ratio[1] and center-of-gravity location,[2] while other parameters were held constant. The results show that the theory overestimates the decay rate of the two-degree-of-freedom hydrofoil model near the critical density ratio, leading to a non-conservative prediction of flutter speed in the range of density ratio of interest for hydrofoils.

In the third investigation[3] of this series of two-degree-of-freedom hydroelastic studies, measured and predicted values of response characteristics and flutter speeds were compared for three models with varying planform characteristics over a range of density ratio. The results show that the non-conservative discrepancy between measured and predicted decay rates and flutter speeds again appears when sweep and taper have been introduced, in the two-degree-of-freedom system. There is, however, no reason to suspect that the qualitative trends predicted by the theory are incorrect. Calculated values of flutter speed based on two-dimensional strip theory for the two-degree-of-freedom model show that increasing sweep angle or decreasing taper yields higher flutter speeds as well as higher values of critical density ratio.

The investigation of measured and predicted response characteristics and flutter speeds is extended in the present study to include the effects of three-dimensional flow with the basic two-degree-of-freedom system used in the first three investigations.[1,2,3] Measured flutter speeds are compared, in this report, with flutter speeds predicted by two-dimensional strip theory, as well as with those predicted by means of three-dimensional lifting-surface theory.[4,5,6] The difficulties encountered in solving the double integral equation, which arises in lifting-surface theory, are discussed. Methods of alleviating these problems are suggested, so that accurate predictions of hydroelastic response characteristics can be obtained for hydrofoils of finite aspect ratio.

Computations were carried out in part at The Computer Center of Stevens Institute of Technology, which is partly supported by the National Science Foundation.

THEORETICAL ANALYSES

EQUATIONS OF MOTION

The equations of motion for a two-degree-of-freedom conservative system with generalized coordinates $q_1(t)$ and $q_2(t)$ can be written[3]

$$\sum_{\ell=1}^{2} M_{j\ell}\, \ddot{q}_{\ell}(t) + \omega_j^{\,2}\, M_{jj} q_j(t) \;=\; Q_j(t);\; j = 1,2 \tag{1}$$

where the generalized masses $M_{j\ell}$ are obtained from the distribution of mass, $m(x,y)$, which participates in the motion through

$$M_{j\ell} \;=\; \iint_H m(x,y)\; f_{\ell}(x,y)\; f_j(x,y)\; dxdy \tag{2}$$

and where the generalized forces Q_j in the present study are obtained, from the unsteady hydrodynamic pressure distribution $\Delta p(x,y,t)$ due to the unsteady motion, by

$$Q_j \;=\; \iint_H \Delta p(x,y,t)\; f_j(x,y)\; dxdy \tag{3}$$

and where ω_j is the uncoupled natural frequency of vibration in the j^{th} degree of freedom in vacuum. In Equations (2) and (3), $f_j(x,y)$ is the mode shape of displacement in the j^{th} degree of freedom, and the range of integration is taken over the hydrofoil planform area, H .

For the particular configuration of this investigation, the generalized coordinates q_1 and q_2 are selected as the translational displacement of the rotational axis of the foil and the rotational displacement about this axis, respectively — both measured at the root section of the foil.

The displacement of any point on the foil is then

$$Z(x,y)T(t) = \sum_{j=1}^{2} f_j(x,y)q_j(t) \tag{4}$$

where mode shapes are taken as

$$f_j(x,y) = \begin{cases} 1.0 & ; j = 1 \\ -x + b_o e_o & ; j = 2 \end{cases} \tag{5}$$

in which b_o is the semichord at the root of the foil and e_o is the distance from the y-axis to the rotational axis in semichords, positive if the rotational axis is aft, as shown in Figure 1.

When one combines Equations (5) and (2), it becomes apparent that

$$\begin{aligned} M_{11} &= M \\ M_{12} &= M_{21} = - b_o x_\alpha M \\ M_{22} &= b_o^2 \, r_\alpha^2 M \end{aligned} \tag{6}$$

where M is the total mass, x_α is the distance in semichords from the rotational axis to the center-of-gravity location, and r_α is the radius of gyration about the rotational axis, in semichords.

Now the introduction of Equations (5) and (6) into the equations of motion (1) leads to

$$M\ddot{q}_1 - x_\alpha b_o M\ddot{q}_2 + \omega_1^2 M q_1 = Q_1 \tag{7}$$

and

$$- x_\alpha b_o M\ddot{q}_1 + b_o^2 \, r_\alpha^2 \, M\ddot{q}_2 + \omega_2^2 \, b_o^2 \, r_\alpha^2 \, M q_2 = Q_2 \tag{8}$$

To proceed further with the solution of these equations, it is necessary to choose a method of representation for the unsteady hydrodynamic pressure distribution $\Delta p(x,y,t)$. Two of the available methods lead to entirely equivalent solutions.

The first method is used for flutter-speed predictions. The time dependence in Equations (7) and (8) is required to be harmonic; then the hydrodynamic pressure $\Delta p(x,y,t)$ can be determined by means of the harmonic pressure-response functions which, in effect, correspond to pressure responses due to unit amplitude oscillations in each degree of freedom. The flutter speed can then be found from the equations of motion. The harmonic-response technique is used in the next section of this report to predict the flutter speeds for the experimental configurations.

The second available method of describing the unsteady hydrodynamic loads is by the use of indicial pressure-response functions which are the responses to unit step changes in downwash in each degree of freedom. The actual pressure response can then be described by means of the Duhamel superposition technique. By introducing harmonic time dependence, this procedure becomes identical with the harmonic-response technique. The indicial response functions will be used subsequently to study the critical value of density ratio for the two-degree-of-freedom system.

FLUTTER ANALYSIS

Harmonic time dependence is introduced in Equations (7) and (8) by

$$\begin{aligned} q_j(t) &= \bar{q}_j(\omega)e^{i\omega t}; \; j=1,2 \\ \Delta p(x,y,t) &= \overline{\Delta p}\,(x,y,\omega)e^{i\omega t} \qquad (9) \\ Q_j(t) &= \bar{Q}_j(\omega)e^{i\omega t}; \; j=1,2 \end{aligned}$$

where the barred quantities are the complex amplitudes of the respective functions at the unknown frequency ω . After cancelling the common factor $e^{i\omega t}$, Equations (7) and (8) become

$$(\omega_1^2 - \omega^2)M\bar{q}_1(\omega) + \omega^2 x_\alpha b_o M\bar{q}_2(\omega) = \bar{Q}_1(\omega) \tag{10}$$

$$\omega^2 x_\alpha M\bar{q}_1(\omega) + (\omega_2^2 - \omega^2)b_o^2\ r_\alpha^2\ M\bar{q}_2(\omega) = \bar{Q}_2(\omega) \tag{11}$$

(Equations [10] and [11] could also be obtained from the Fourier transform of Equations [7] and [8].)

The unknown pressure $\overline{\Delta p}(x,y,\omega)$ is expressed in terms of the harmonic pressure responses $\bar{p}_j(x,y,\omega)$ for a unit amplitude translational oscillation $(j = 1)$ or rotational oscillation $(j = 2)$, by

$$\overline{\Delta p}(x,y,\omega) = \sum_{j=1}^{2} \bar{p}_j(x,y,\omega)\ \bar{q}_j(\omega) \tag{12}$$

Several methods are available for calculating these harmonic-response functions, $\bar{p}_j$. However, the most accurate one for three-dimensional-flow conditions employs lifting-surface theory, in which the response functions are related to the displacement by the integral equation[4,5]

$$(i\omega + U\frac{\partial}{\partial x})\ f_j(x,y) = \frac{1}{4\pi\rho U}\int_H\int \bar{p}_j(\xi,\eta,\omega)\ K(x,y;\xi,\eta;\omega)\ d\xi d\eta \tag{13}$$

where the kernel function K is taken as presented by Watkins, Woolston, and Cunningham[4] for infinite fluid. (The corresponding kernel function for operation near a free surface at arbitrary Froude number has been derived by Tsakonas and Henry.[5]) Substituting Equation (5) for $f_j(x,y)$ in Equation (13), yields

$$i\omega = \frac{1}{4\pi\rho U}\int_H\int \bar{p}_1(\xi,\eta,\omega)\ K(x,y;\xi,\eta;\omega)\ d\xi d\eta \tag{14}$$

and

$$i\omega(-x + b_o e_o) - U = \frac{1}{4\pi\rho U} \int_H \int \bar{p}_2(\xi,\eta,\omega)\ K(x,y;\xi,\eta;\omega)\ d\xi d\eta \tag{15}$$

But $\bar{p}_2$ can be considered as a linear combination of the responses to each term on the left-hand side of Equation (15). This gives

$$-\ i\omega x = \frac{1}{4\pi\rho U} \int_H \int \bar{p}_2^{\,*}(\xi,\eta,\omega)\ K(x,y;\xi,\eta;\omega)\ d\xi d\eta \tag{16}$$

$$i\omega b_o e_o = \frac{1}{4\pi\rho U} \int_H \int \bar{p}_2^{\,(1)}(\xi,\eta,\omega)\ K(x,y;\xi,\eta;\omega)\ d\xi d\eta \tag{17}$$

$$-\ U = \frac{1}{4\pi\rho U} \int_H \int \bar{p}_2^{\,(2)}(\xi,\eta,\omega)\ K(x,y;\xi,\eta;\omega)\ d\xi d\eta \tag{18}$$

and then

$$\bar{p}_2(\xi,\eta,\omega) = \bar{p}_2^{\,*} + \bar{p}_2^{\,(1)} + \bar{p}_2^{\,(2)} \tag{19}$$

Comparing Equations (17) and (18) with Equation (14), we see that

$$\bar{p}_2^{\,(1)} = b_o e_o \bar{p}_1 \tag{20}$$

and

$$\bar{p}_2^{\,(2)} = -\frac{U}{i\omega}\,\bar{p}_1 \tag{21}$$

Then, from Equation (19),

$$\bar{p}_2(\xi,\eta,\omega) = \bar{p}_2^{\,*} + \left(\frac{iU}{\omega} + b_o e_o\right)\bar{p}_1 \tag{22}$$

Combining Equations (12) and (22) gives

$$\overline{\Delta p}(x,y,\omega) = \bar{p}_1(x,y,\omega)\bar{q}_1(\omega) + \left[\bar{p}_2^{*}(x,y,\omega) + \left(\frac{iU}{\omega} + b_o e_\alpha\right)\bar{p}_1(x,y,\omega)\right]\bar{q}_2(\omega)$$

(23)

where the harmonic-response functions $\bar{p}_1$ and $\bar{p}_2^{*}$ are found from the integral Equations (14) and (16). Equation (23) is the desired representation of the unknown pressure distributor $\overline{\Delta p}$ in terms of the harmonic-response functions $\bar{p}_1$ and $\bar{p}_2^{*}$.

The equations of motion (10) and (11) are now put in dimensionless form by dividing by $\pi\rho b_o^3\omega^2 s$ and $\pi\rho b_o^4\omega^2 s$, respectively. This gives

$$\left[\left(\frac{\omega_1}{\omega}\right)^2 - 1\right]\mu\frac{\bar{q}_1}{b_o} + x_\alpha\mu\bar{q}_2 = \frac{\bar{Q}_1}{\pi\rho b_o^3\,\omega^2 s} \tag{24}$$

and

$$x_\alpha\mu\frac{\bar{q}_1}{b_o} + \left[\left(\frac{\omega_2}{\omega}\right)^2 - 1\right]r_\alpha^2\mu\bar{q}_2 = \frac{\bar{Q}_2}{\pi\rho b_o^4\,\omega^2 s} \tag{25}$$

where s is the span of the model and μ is the density ratio defined by

$$\mu = \frac{M}{\pi\rho b_o^2 s} \tag{26}$$

In the present study, the rotational axis is parallel to the y-axis, so that e_o is constant along the span.

The hydrodynamic forces in Equations (24) and (25) can be written in terms of the three-dimensional harmonic hydrodynamic derivatives, which are defined by

$$L_{11} = \iint_H \frac{\bar{p}_1(x,y,\omega)}{\pi\rho b_o\omega^2}\, d\frac{x}{b_o}\, d\frac{y}{s}$$

[Cont'd]

$$L_{12} = \iint_H \frac{\bar{p}_2^*(x,y,\omega)}{\pi\rho b_o^2\omega^2} \, d\frac{x}{b_o} \, d\frac{y}{s} + \frac{i}{k} L_{11}$$

$$L_{21} = -\iint_H \frac{x}{b_o} \frac{\bar{p}_1(x,y,\omega)}{\pi\rho b_o\omega^2} \, d\frac{x}{b_o} \, d\frac{y}{s} \tag{27}$$

$$L_{22} = -\iint_H \frac{x}{b_o} \frac{\bar{p}_2^*(x,y,\omega)}{\pi\rho b_o^2\omega^2} \, d\frac{x}{b_o} \, d\frac{y}{s} + \frac{i}{k} L_{21}$$

where $k = \omega b_o/U$ is the reduced frequency and where the harmonic-response operators are found from the dimensionless forms of Equations (14) and (16), which become

$$\frac{4i}{k} = \iint_H \frac{\bar{p}_1(\xi,\eta)}{\pi\rho b_o\omega^2} \, b_o s \; K(x,y;\xi,\eta;\omega) \tag{28}$$

and

$$\frac{-4i}{k} \; \frac{x}{b_o} = \iint_H \frac{\bar{p}_2^*}{\pi\rho b_o^2\omega^2} \, b_o s K(x,y;\xi,\eta;\omega) \; d\xi d\eta \tag{29}$$

The dimensionless generalized forces are then given by

$$\frac{\bar{Q}_1}{\pi\rho b_o^3\omega^2 s} = \frac{\bar{q}_1}{b_o} L_{11} + \bar{q}_2(L_{12} + e_o L_{11}) \tag{30}$$

$$\frac{\bar{Q}_2}{\pi\rho b_o^4\omega^2 s} = \frac{\bar{q}_1}{b_o} (L_{21} + e_o L_{11}) + \bar{q}_2 \left[L_{22} + e_o(L_{21} + L_{12}) + e_o^2 L_{11} \right] \tag{31}$$

so that the equations of motion can be written in the homogeneous form

$$\frac{\bar{q}_1}{b_o}\left\{\left[1-\left(\frac{\omega_1}{\omega_2}\right)^2\left(\frac{\omega_2}{\omega}\right)^2\right]\mu+L_{11}\right\}+\bar{q}_2\left\{-\mu x_\alpha+L_{12}+e_oL_{11}\right\}=0 \tag{32}$$

$$\frac{\bar{q}_1}{b_o}\left\{-\mu x_\alpha+L_{21}+e_oL_{11}\right\}+\bar{q}_2\left\{\left[1-\left(\frac{\omega_2}{\omega}\right)^2\right]\mu r_\alpha^2+L_{22}+e_o(L_{21}+L_{12})+e_o^2L_{11}\right\}=0 \tag{33}$$

For a non-trivial solution of Equations (32) and (33), it is required that the determinant of the coefficients vanish, to yield the flutter determinant

$$\begin{vmatrix} \left[1-\left(\frac{\omega_1}{\omega_2}\right)^2\left(\frac{\omega_2}{\omega}\right)^2\right]\mu+L_{11} & -\mu x_\alpha+L_{12}+e_oL_{11} \\ -\mu x_\alpha+L_{21}+e_oL_{11} & \left[1-\left(\frac{\omega_2}{\omega}\right)^2\right]\mu r_\alpha^2+L_{22} \\ & +e_o(L_{21}+L_{12})+e_o^2L_{11} \end{vmatrix}=0 \tag{34}$$

The solution of Equation (34) for the unknowns k and ω_2/ω is obtained by letting μ be an unknown for specified values of k. The flutter speed can then be determined, at each k, from

$$\frac{U_F}{b\omega_2}=\frac{1}{k\left(\frac{\omega_2}{\omega}\right)} \tag{35}$$

However, the evaluation of the three-dimensional harmonic hydrodynamic derivatives in Equation (34) is in itself a major undertaking, for which two methods are here presented. The first method utilizes two-dimensional flow results in a stripwise manner, and the second method utilizes the numerical solution of the integral equations (28) and (29).

Two-Dimensional Stripwise Technique

If the span of the hydrofoil is large, and if the mode shapes, rotational axis location, and planform geometry change slowly in the spanwise direction, then the hydrodynamic force and moment per unit span can be closely approximated by those of two-dimensional hydrofoil sections with the same properties at each spanwise station. This approximation was carried out earlier by the authors,[3] and it was shown that the flutter determinant (34) reduces to

$$\begin{vmatrix} \mu\left[1 - \left(\frac{\omega_1}{\omega_2}\right)^2 \left(\frac{\omega_2}{\omega}\right)^2\right] + F_h & -\mu x_\alpha + F_\alpha \\ -\mu x_\alpha + T_h & \mu r_\alpha^2\left[1 - \left(\frac{\omega_2}{\omega}\right)^2\right] + T_\alpha \end{vmatrix} = 0 \qquad (36)$$

In the earlier work,[3] the authors also presented the procedure for solving this equation as well as expressions for the hydrodynamic forces $F_h, \ldots, T_\alpha$, in terms of the Theodorsen function $C(k)$.

Three-Dimensional Lifting-Surface Theory

In order to utilize the three-dimensional harmonic representation of the unsteady hydrodynamic forces, the integral equations (28) and (29) are solved numerically and the three-dimensional harmonic hydrodynamic derivatives are evaluated by means of Equation (27). These integral equations are of the form

$$w'(x,y) = \iint p'(\xi,\eta) K'(x,y;\xi,\eta)\, d\xi d\eta \qquad (37)$$

where w' and p' are the dimensionless downwash and pressure distributions and K' is the dimensionless kernel function given by[4]

$$K'(x,y;\xi,\eta) = \frac{1}{(y-\eta)^2}\,\frac{x-\xi}{\sqrt{(x-\xi)^2+(y-\eta)^2}} + \frac{e^{-ik(x-\xi)}}{(y-\eta)^2}\Bigg\{-ik|y-\eta| + k|y-\eta|\,K_1(k|y-\eta|) + i\frac{\pi}{2}k|y-\eta| \cdot\Big[I_1(k|y-\eta|) - L_1(k|y-\eta|)\Big] - ik|y-\eta|\int_0^{\frac{x-\xi}{|y-\eta|}} \frac{\tau e^{ik|y-\eta|\tau}}{\sqrt{1+\tau^2}}\,d\tau\Bigg\} \tag{38}$$

where $K_1(z)$, $I_1(z)$, and $L_1(z)$ are the first-order modified Bessel functions, of the first and second kind, and the modified Struve function, respectively. The numerical procedure for evaluating K' and for solving Equation (37), as described by Watkins et al.,[4] has been programmed for use in this investigation. The flutter speed can then be found from Equation (35) in conjunction with (27) and (34), once the solution of the integral equations (28) and (29) are obtained at the chosen value of reduced frequency. The numerical work, however, is quite complicated and requires extreme accuracy. These points are discussed at greater length in another section.

QUASI-STEADY ANALYSIS FOR CRITICAL DENSITY RATIO

In earlier flutter analyses,[1,2,3,5,6] the flutter speed was found to have asymptotic behavior for density ratios, μ, in the range of practical interest for hydrofoils. Along this branch of the flutter-speed curve, one finds that $k \rightarrow 0$ as $U_F \rightarrow \infty$. As a result, the critical value of density ratio, μ_{CR}, at which the asymptote occurs, can be predicted by using the quasi-steady approximation of the circulatory lift. (If the added mass is neglected as well, i.e., $k = 0$ in the equations of motion, the resulting solution gives the static divergence speed.) Applying the limit $k \to 0$ to the circulatory parts of Equations (27), or in the integral equations (28) and (29), is a cumbersome task because the added mass and circulatory parts are not easily separated. With the indicial response functions, however, this separation is very easily introduced; therefore a method for predicting μ_{CR}, using these functions, is presented here.

The unknown pressure $\Delta p(x,y,t)$, with arbitrary time dependence, is related to a displacement $Z(x,y)T(t)$ by the integral equation[6]

$$\left(\frac{\partial}{\partial t} + U\frac{\partial}{\partial x}\right) Z(x,y)T(t) = \frac{1}{4\pi\rho}\int_{-\infty}^{t} d\tau \int_H\int \Delta p(\xi,\eta,\tau)\, K_1(x,y;t;\xi,\eta,\tau)\, d\xi d\eta \tag{39}$$

where K_1 is the kernel function derived by Drischler.[7] (The corresponding kernel function for operation near a free surface at arbitrary Froude number is derived in an earlier work by Henry.[6])

Because of the linear properties of the governing equations of the system, the total pressure response Δp can be divided into a component $\Delta p^{(t)}$ due to the downwash $Z\partial T/\partial t$ and a component $\Delta p^{(x)}$ due to $UT\partial Z/\partial x$ These two components of pressure are then the solutions of the integral equations

$$Z\partial T/\partial t = \frac{1}{4\pi\rho}\int_{-\infty}^{t} d\tau \int_H\int \Delta p^{(t)}(\xi,\eta,\tau)\, K_1(x,y,t;\xi,\eta,\tau)\, d\xi d\eta \tag{40}$$

$$UT\partial Z/\partial x = \frac{1}{4\pi\rho}\int_{-\infty}^{t} d\tau \int_H\int \Delta p^{(x)}(\xi,\eta,\tau)\, K_1(x,y,t;\xi,\eta,\tau)\, d\xi d\eta \tag{41}$$

One could proceed to solve these integral equations numerically. A more fruitful procedure, however, is first to find the corresponding indicial response functions $p_i^{(t)}$ and $p_i^{(x)}$ and then obtain a representation for Δp through the Duhamel superposition principle.

To find the indicial response functions, the time dependence on the left-hand sides of Equations (40) and (41) is replaced by the unit step function $H_1(t)$, and the functions $p_i^{(t)}$ and $p_i^{(x)}$ are divided into added-mass, quasi-steady, and unsteady components,[6] such that

$$p_i^{(t)}(x,y,t) = p_{NC}^{(t)}(x,y)\delta(t) + p_{QS}^{(t)}(x,y)H_1(t) + p_{US}^{(t)}(x,y,t)$$

and (42)

$$p_i^{(x)}(x,y,t) = p_{NC}^{(x)}(x,y)\delta(t) + p_{QS}^{(x)}(x,y)H_1(t) + p_{US}^{(x)}(x,y,t)$$

where $\delta(t)$ is the Dirac delta function and $H_1(t)$ is the unit step function. In this analysis to find μ_{CR}, we are only interested in the non-circulatory and quasi-steady parts of the lift; hence it is assumed that $p_{US}^{(t)}$ and $p_{US}^{(x)}$ are zero for all time. Then Equation (42) can be rewritten as

$$p_i^{(t)}(x,y,t) = p_{NC}^{(t)}(x,y)\delta(t) + p_{QS}^{(t)}(x,y)H_1(t)$$

(43)

$$p_i^{(x)}(x,y,t) = p_{NC}^{(x)}(x,y)\delta(t) = p_{QS}^{(x)}(x,y)H_1(t)$$

The integral equations for the indicial response functions are then

$$Z(x,y)H_1(t) = \frac{1}{4\pi\rho}\int_{-\infty}^{t} d\tau \int_H\int \left[p_{NC}^{(t)}(\xi,\eta)\delta(\tau) + p_{QS}^{(t)}(\xi,\eta)H_1(\tau)\right] K_1 \, d\xi d\eta \tag{44}$$

$$U\, H_1(t)\, \frac{\partial Z(x,y)}{\partial x} = \frac{1}{4\pi\rho}\int_{-\infty}^{t} d\tau \int_H\int \left[p_{NC}^{(x)}(\xi,\eta)\delta(\tau) + p_{QS}^{(x)}(\xi,\eta)H_1(\tau)\right] K_1 \, d\xi d\eta \tag{45}$$

At $t = 0^+$, Equations (44) and (45) yield

$$Z(x,y) = \frac{1}{4\pi\rho}\int_H\int p_{NC}^{(t)}(\xi,\eta)\; K_1(x,y,0;\xi,\eta,0)\; d\xi d\eta \tag{46}$$

$$U\,\frac{\partial Z(x,y)}{\partial x} = \frac{1}{4\pi\rho}\int_H\int p_{NC}^{(x)}(\xi,\eta)\; K_1(x,y,0;\xi,\eta,0)\; d\xi d\eta \tag{47}$$

whereas when $t \to \infty$ they reduce to

$$Z(x,y) = \frac{1}{4\pi\rho} \iint_H p_{QS}^{(t)}(\xi,\eta) \lim_{t\to\infty} \int_0^t K_1(x,y,t;\xi,\eta,\tau)\, d\tau\, d\xi\, d\eta \qquad (48)$$

$$U \frac{\partial Z(x,y)}{\partial x} = \frac{1}{4\pi\rho} \iint_H p_{QS}^{(x)}(\xi,\eta) \lim_{t\to\infty} \int_0^t K_1(x,y,t;\xi,\eta,\tau)\, d\tau\, d\xi\, d\eta \qquad (49)$$

The necessary components of the indicial pressure-response functions can be found from these four integral equations. By introducing the Duhamel superposition principle, an expression for the quasi-steady and added-mass contributions to the actual pressure response due to the time dependence of the motion $T(t)$ is obtained.

$$\Delta p(x,y,t) = \int_{-\infty}^t p_i^{(t)}(x,y,t-\tau) \frac{\partial^2 T}{\partial \tau^2}(\tau)\, d\tau + \int_{-\infty}^t p_i^{(x)}(x,y,t-\tau) \frac{\partial T}{\partial \tau}(\tau)\, d\tau$$

$$= p_{NC}^{(t)}(x,y) \int_{-\infty}^t \delta(t-\tau) \frac{\partial^2 T}{\partial \tau^2}(\tau)\, d\tau + p_{NC}^{(x)}(x,y) \int_{-\infty}^t \delta(t-\tau) \frac{\partial T}{\partial \tau}(\tau)\, d\tau$$

$$+ p_{QS}^{(t)}(x,y) \int_{-\infty}^t H_1(t-\tau) \frac{\partial^2 T}{\partial \tau^2}(\tau)\, d\tau + p_{QS}^{(x)}(x,y) \int_{-\infty}^t H_1(t-\tau) \frac{\partial T}{\partial \tau}(\tau)\, d\tau$$

Carrying out the indicated operations leads to

$$\Delta p(x,y,t) = p_{NC}^{(t)}(x,y)\ddot{T}(t) + p_{NC}^{(x)}(x,y)\dot{T}(t) + p_{QS}^{(t)}(x,y)\dot{T}(t) + p_{QS}^{(x)}(x,y)T(t) \qquad (50)$$

The above procedure is applied to the two-degree-of-freedom system by introducing Equation (4) into Equations (46) through (50), and dividing the indicial pressure responses into components for each mode of displacement. This gives

$$f_j(x,y) = \frac{1}{4\pi\rho} \iint_H p_{NCj}^{(t)}(\xi,\eta)\; K_1(x,y,0;\xi,\eta,0)\; d\xi d\eta;\; j=1,2 \tag{51}$$

$$U\frac{\partial f_j}{\partial x}(x,y) = \frac{1}{4\pi\rho} \iint_H p_{NCj}^{(x)}(\xi,\eta)\; K_1(x,y,0;\xi,\eta,0)\; d\xi d\eta;\; j=1,2 \tag{52}$$

$$f_j(x,y) = \frac{1}{4\pi\rho} \iint_H p_{QSj}^{(t)}(\xi,\eta)\; \lim_{t\to\infty} \int_0^t K_1(x,y,t;\xi,\eta,\tau)\; d\tau d\eta;\; j=1,2 \tag{53}$$

$$U\frac{\partial f_j}{\partial x}(x,y) = \frac{1}{4\pi\rho} \iint_H p_{QSj}^{(x)}(\xi,\eta)\; \lim_{t\to\infty} \int_0^t K_1(x,y,t;\xi,\eta,\tau)\; d\tau d\xi d\eta;\; j=1,2 \tag{54}$$

$$\Delta p(x,y,t) = \sum_{j=1}^{2} \Big[p_{NCj}^{(t)}(x,y)\ddot{q}_j(t) + p_{NCj}^{(x)}(x,y)\dot{q}_j(t) + p_{QSj}^{(t)}(x,y)\dot{q}_j(t) + p_{QSj}^{(x)}(x,y)q_j(t) \Big] \tag{55}$$

Many simplifications arise when Equation (5) is used in Equations (51) through (55), leading to

$$1.0 = \frac{1}{4\pi\rho} \iint_H p_{NC1}^{(t)}\; K_1(x,y,0;\xi,\eta,0)\; d\xi d\eta \tag{56a}$$

$$-x+b_o e_o = \frac{1}{4\pi\rho} \iint_H p_{NC2}^{(t)}\; K_1(x,y,0;\xi,\eta,0)\; d\xi d\eta \tag{56b}$$

$$0 = \frac{1}{4\pi\rho} \iint_H p_{NC1}^{(x)} \; K_1(x,y,0;\xi,\eta,0) \; d\xi d\eta \tag{56c}$$

$$-U = \frac{1}{4\pi\rho} \iint_H p_{NC2}^{(x)} \; K_1(x,y,0;\xi,\eta,0) \; d\xi d\eta \tag{56d}$$

$$1.0 = \frac{1}{4\pi\rho} \iint_H p_{QS1}^{(t)} \lim_{t\to\infty} \int_o^t K_1(x,y,t;\xi,\eta,\tau) \; d\tau d\xi d\eta \tag{56e}$$

$$-xb_o e_o = \frac{1}{4\pi\rho} \iint_H p_{QS2}^{(t)} \lim_{t\to\infty} \int_o^t K_1(x,y,t;\xi,\eta,\tau) \; d\tau d\xi d\eta \tag{56f}$$

$$0 = \frac{1}{4\pi\rho} \iint_H p_{QS1}^{(x)} \lim_{t\to\infty} \int_o^t K_1(x,y,t;\xi,\eta,\tau) \; d\tau d\xi d\eta \tag{56g}$$

$$-U = \frac{1}{4\pi\rho} \iint_H p_{QS2}^{(x)} \lim_{t\to\infty} \int_o^t K_1(x,y,t;\xi,\eta,\tau) \; d\tau d\xi d\eta \tag{56h}$$

From Equations (56c) and (56g), we see that

$$p_{NC1}^{(x)} = p_{QS1}^{(x)} = 0$$

while from other similar comparisons we find that

$$p_{NC2}^{(t)} = p_{NC2}^{(t)*} + b_o e_o p_{NC1}^{(t)}$$

$$p_{NC2}^{(x)} = -U p_{NC1}^{(t)}$$

$$p_{QS2}^{(t)} = p_{QS2}^{(t)*} + b_o e_o p_{QS1}^{(t)}$$

$$p_{QS2}^{(x)} = -U p_{QS1}^{(t)}$$

where $p_{NC2}^{(t)*}$ and $p_{QS2}^{(t)*}$ are the solutions of

$$-x = \frac{1}{4\pi\rho} \iint_H p_{NC2}^{(t)*} K_1(x,y,0;\xi,\eta,0)\, d\xi d\eta \tag{57a}$$

and

$$-x = \frac{1}{4\pi\rho} \iint_H \dot{p}_{QS2}^{(t)*} \lim_{t\to\infty} \int_{-\infty}^{t} K_1(x,y,t;\xi,\eta,\tau)\, d\tau d\xi d\eta \tag{57b}$$

The quasi-steady pressure response for the two-degree-of-freedom system, Equation (55), now reduces to

$$\Delta p(x,y,t) = p_{NC1}^{(t)}\ddot{q}_1 + p_{QS1}^{(t)}\dot{q}_1 + \left[p_{NC2}^{(t)*} + b_o e_o p_{NC1}^{(t)}\right]\ddot{q}_2 - U p_{NC1}^{(t)}\dot{q}_2$$

$$+ \left[p_{QS2}^{(t)*} + b_o e_o p_{QS1}^{(t)}\right]\dot{q}_2 - U p_{QS1}^{(t)} q_2 \tag{58}$$

where the four indicial response operators $p_{NC1}^{(t)}$, $p_{QS1}^{(t)}$, $p_{NC2}^{(t)*}$, and $p_{QS2}^{(t)*}$ are obtained from the integral equations (56a), (56e), (57a), and (57b), respectively.

The corresponding generalized forces are found by inserting Equation (58) into Equation (3). In the resulting expressions, the dimensionless quasi-steady and added-mass indicial derivatives are defined by

$$L_{\ddot{q}_1} = -\iint_H \frac{p_{NC1}^{(t)}}{\rho b_o}\, d\frac{x}{b_o}\, d\frac{y}{s}, \qquad M_{\ddot{q}_1} = \iint_H \frac{x}{b_o}\frac{p_{NC1}^{(t)}}{\rho b_o}\, d\frac{x}{b_o}\, d\frac{y}{s}$$

$$L_{\dot{q}_1} = \iint_H \frac{p_{QS1}^{(t)}}{\rho U}\, d\frac{x}{b_o}\, d\frac{y}{s}, \qquad M_{\dot{q}_1} = -\iint_H \frac{x}{b_o}\frac{p_{QS1}^{(t)}}{\rho U}\, d\frac{x}{b_o}\, d\frac{y}{s} \tag{59}$$

$$L_{\ddot{q}_2} = -\iint_H \frac{p_{NC2}^{(t)*}}{\rho U b_o^2}\, d\frac{x}{b_o}\, d\frac{y}{s}, \qquad M_{\ddot{q}_2} = \iint_H \frac{x}{b_o}\frac{p_{NC2}^{(t)*}}{\rho U b_o^2}\, d\frac{x}{b_o}\, d\frac{y}{s}$$

[Cont'd]

$$L_{\dot{q}_2} = \iint\limits_H \frac{p_{QS2}^{(t)*}}{\rho U b_o}\, d\frac{x}{b_o}\, d\frac{y}{s}\,, \qquad M_{\dot{q}_2} = -\iint\limits_H \frac{x}{b_o}\, \frac{p_{QS2}^{(t)*}}{\rho U b_o}\, d\frac{x}{b_o}\, d\frac{y}{s}$$

Combining Equations (3), (5), (58), and (59) then leads to

$$\frac{Q_1}{\rho U^2 b_o s} = -L_{\ddot{q}_1}\ddot{q}_1 + L_{\dot{q}_1}\dot{q}_1 - (L_{\ddot{q}_2} + e_o L_{\ddot{q}_1})\ddot{q}_2 + (L_{\dot{q}_2} + L_{\ddot{q}_1} + e_o L_{\dot{q}_1})\dot{q}_2 - L_{\dot{q}_1} q_2 \tag{60}$$

$$\begin{aligned}\frac{Q_2}{\rho U^2 b_o^2 s} = &-(M_{\ddot{q}_1} + e_o L_{\ddot{q}_1})\ddot{q}_1 + (M_{\dot{q}_1} + e_o L_{\dot{q}_1})\dot{q}_1 - \left[M_{\ddot{q}_2} + e_o(M_{\ddot{q}_1} + L_{q_2}) + e_o^2 L_{\ddot{q}_1}\right]\ddot{q}_2 \\ &+ \left[M_{\dot{q}_2} + M_{\ddot{q}_1} + e_o(M_{\dot{q}_1} + L_{\dot{q}_2} + L_{\ddot{q}_1}) + e_o^2 L_{\dot{q}_1}\right]\dot{q}_2 - (M_{\dot{q}_1} + e_o L_{\dot{q}_1}) q_2\end{aligned} \tag{61}$$

Dividing Equations (7) and (8) by $\rho U^2 b_o s$ and $\rho U^2 b_o{}^2 s$ respectively, and introducing Equations (60) and (61), yields the homogeneous quasi-steady equations of motion

$$\begin{aligned}&(\pi\mu + L_{\ddot{q}_1})\ddot{q}_1 - L_{\dot{q}_1}\dot{q}_1 + \pi\mu\left(\frac{\omega_1}{\omega_2}\right)^2 \Omega^2 q_1 + (-\pi\mu x_\alpha + L_{\ddot{q}_2} + e_o L_{\ddot{q}_1})\ddot{q}_2 \\ &\qquad -(L_{\dot{q}_2} + L_{\ddot{q}_1} + e_o L_{q_1})\dot{q}_2 + L_{\dot{q}_1} q_2 = 0\end{aligned} \tag{62}$$

$$\begin{aligned}&(-\pi\mu x_\alpha + M_{\ddot{q}_1} + e_o L_{\ddot{q}_1})\ddot{q}_1 - (M_{\dot{q}_1} + e_o L_{\dot{q}_1})\dot{q}_1 + \left[\pi\mu r_\alpha^2 + M_{\ddot{q}_2} + e_o(M_{\dot{q}_1} + L_{\ddot{q}_2}) + e_o^2 L_{\ddot{q}}\right]\ddot{q}_2 \\ &- \left[M_{\dot{q}_2} + M_{\ddot{q}_1} + e_o(M_{\dot{q}_1} + L_{\dot{q}_2} + L_{\ddot{q}_1}) + e_o^2 L_{\dot{q}_1}\right]\dot{q}_2 + (\pi\mu r_\alpha^2 \Omega^2 + M_{q_1} + e_o L_{\dot{q}_1}) q_2 = 0\end{aligned} \tag{63}$$

where $\Omega = \omega_2 b/U$. Introducing the Fourier transform as

$$\bar{F}(k) = \frac{1}{2\pi}\int_{-\infty}^{\infty} F(t) e^{-ikt} dt \tag{64}$$

where t is the dimensionless time and k is the reduced frequency, the transforms of the equations of motion (62) and (63) are then reduced to the homogeneous algebraic equations

$$\left[-k^2(\pi\mu + L_{\ddot{q}_1}) - ikL_{\dot{q}_1} + \pi\mu\left(\frac{\omega_1}{\omega_2}\right)^2 \Omega^2\right]\bar{q}_1 +$$

$$\left[-k^2(-\pi\mu x_\alpha + L_{\ddot{q}_2} + e_o L_{\ddot{q}_1}) - ik(L_{\dot{q}_2} + L_{\ddot{q}_1} + e_o L_{\dot{q}_1}) + L_{\dot{q}_1}\right]\bar{q}_2 = 0 \tag{65}$$

$$\left[-k^2(-\pi\mu x_\alpha + M_{\ddot{q}_1} + e_o L_{\ddot{q}_1}) - ik(M_{\dot{q}_1} + e_o L_{\dot{q}_1})\right]\bar{q}_1 + \left\{-k^2\left[\pi\mu r_\alpha^2 + M_{\ddot{q}_2} + e_o(M_{\ddot{q}_1} + L_{\ddot{q}_2}) e_o^2 L_{\ddot{q}_1}\right]\right.$$

$$\left. -ik\left[M_{\dot{q}_2} + M_{\ddot{q}_1} + e_o(M_{q_1} + L_{\dot{q}_2} + L_{\ddot{q}_1}) + e_o^2 L_{q_1}\right] + (\pi\mu r_\alpha^2 \Omega^2 + M_{\dot{q}_1} + e_o L_{\dot{q}_1})\right\}\bar{q}_2 = 0 \tag{66}$$

A non-trivial solution of these equations for $\bar{q}_1$ and $\bar{q}_2$ exists only if the determinant of their coefficients vanishes. The expansion of this determinant leads to a fourth-order characteristic polynomial in k. Expressions for the two unknown Ω and k in Equations (65) and (66) can then be found from the real and imaginary parts of the characteristic polynomial.

To find the conditions at which $U_F \to \infty$, an expression for $1/\Omega$ is obtained from the characteristic polynomial and the denominator of this expression is set equal to zero. The resulting equation gives the value of density ratio at which $U_F \to \infty$. This critical value of density ratio is given by

$$\mu_{CR} = \frac{B\left(\frac{\omega_1}{\omega_2}\right)^2 (M_{\dot{q}_1} + e_o L_{\dot{q}_1}) - C(L_{\dot{q}_1} M_{\dot{q}_2} - L_{\dot{q}_2} M_{\dot{q}_1})}{\pi\left[C(M_{\dot{q}_1} + e_o L_{\dot{q}_1} + x_\alpha L_{\dot{q}_1}) - A\left(\frac{\omega_1}{\omega_2}\right)^2 (M_{\dot{q}_1} + e_o L_{\dot{q}_1})\right]} \tag{67}$$

where

$$A = M_{\dot{q}_2} + M_{\ddot{q}_1} + e_o(M_{\dot{q}_1} + L_{q_2} + L_{\ddot{q}_1}) + e_o^2 L_{\dot{q}_1} + r_\alpha^2 L_{\dot{q}_1}$$

$$+ x_\alpha(M_{\dot{q}_1} + L_{\dot{q}_2} + L_{\ddot{q}_1} - 2e_o L_{\dot{q}_1}) + L_{\dot{q}_1} M_{\ddot{q}_2} + L_{\ddot{q}_1} M_{\dot{q}_2} L_{\dot{q}_2} M_{\ddot{q}_1} - L_{\ddot{q}_2} M_{\dot{q}}$$

$$B = - L_{\dot{q}_1} M_{\dot{q}_1} + e_o(L_{\dot{q}_1})^2$$

$$C = r_\alpha^2 L_{q_1} + \left(\frac{\omega_1}{\omega_2}\right)^2 \left[M_{\dot{q}_2} + M_{\ddot{q}_1} + e_o(M_{\dot{q}_1} + L_{\dot{q}_2} + L_{\ddot{q}_1}) + e_o^2 L_{q_1}\right]$$

Here again, as in the flutter analysis, the solution of the equations of motion is straightforward. In contrast, the calculation of the hydrodynamic derivatives appearing in Equation (67) is a major task.

Two-Dimensional Stripwise Technique

The generalized forces have been derived by the two-dimensional stripwise technique in an earlier work by the authors.[3] Expressions for the indicial derivatives defined in Equation (59) can be obtained from the generalized forces given in Equations (43) and (44) of that study. For the case of a hydrofoil with midchord sweep angle Λ, taper ratio T, and span-to-chord ratio A, the indicial derivatives obtained from two-dimensional strip theory are given by

$$L_{\ddot{q}_1} = \frac{\pi(1-T^3)\cos\Lambda}{3(1-T)}$$

$$L_{\dot{q}_1} = \frac{-\pi(1-T^2)\cos\Lambda}{(1-T)}$$

$$L_{\ddot{q}_2} = \frac{-\pi e_o(1-4T^3+3T^4)\cos\Lambda}{12(1-T)} - \frac{\pi A\sin\Lambda(1-5T^4+4T^5)}{20b_o(1-T)^2}$$

$$L_{\dot{q}_2} = L_{\ddot{q}_1} + \frac{\pi e_o(1-3T^2+2T^3)\cos\Lambda}{3(1-T)} + \frac{\pi A\sin\Lambda(1-4T^3+3T^4)}{6b_o(1-T)^2}$$

[Cont'd]

$$M_{\ddot{q}_1} = L_{\ddot{q}_2}$$

$$M_{\dot{q}_1} = - L_{\dot{q}_1} + \frac{\pi e_o (1-3T^2+2T^3)\cos\Lambda}{3(1-T)} + \frac{\pi A \sin\Lambda(1-4T^3+3T^4)}{6b_o(1-T)^2}$$

$$M_{\ddot{q}_2} = \frac{\pi(1-T^5)\cos\Lambda}{40(1-T)} + \frac{\pi e_o^2(1-10T^3+15T^4-6T^5)\cos\Lambda}{30(1-T)}$$

$$+ \frac{\pi e_o A \sin\Lambda(1-15T^4+24T^5-10T^6)}{30b_o(1-T)^2}$$

$$+ \frac{\pi(A \tan\Lambda)^2\cos\Lambda(1-21T^5+35T^6-15T^7)}{105(1-T)^3}$$

$$M_{\dot{q}_2} = - \frac{\pi e_o^2(1-6T^2+8T^3-3T^4)\cos\Lambda}{6(1-T)} - \frac{2\pi e_o A \sin\Lambda(1-10T^3+15T^4-6T^5)}{15b_o(1-T)^2}$$

$$- \frac{\pi(A \tan\Lambda)^2\cos\Lambda(1-15T^4+24T^5-10T^6)}{30(1-T)^3} \qquad (68)$$

Equations (67) and (68) then lead to the two-dimensional strip theory prediction of μ_{CR} .

These results can be reduced to the expression for μ_{CR} in two-dimensional flow[1,2] by letting $T \to 1$ and $\Lambda = 0$. Equations (68) then become

$$\begin{aligned} L_{\ddot{q}_1} &= \pi & M_{\ddot{q}_1} &= 0 \\ L_{\dot{q}_1} &= -2\pi & M_{\dot{q}_1} &= -\pi \\ L_{\ddot{q}_2} &= 0 & M_{\ddot{q}_2} &= \pi/8 \\ L_{\dot{q}_2} &= \pi & M_{\dot{q}_2} &= 0 \end{aligned} \qquad (69)$$

Substituting Equations (69) into Equation (67) leads to

$$\mu_{CR} = \frac{r_\alpha^2 + \left(\frac{\omega_1}{\omega_2}\right)^2 \left(\frac{1}{2}-e_o\right)\left[e_o - 4\left(\frac{1}{2}-e_o\right)\right]}{\left(\frac{1}{2}+e_o+x_\alpha\right)\left[r_\alpha^2 + \left(\frac{\omega_1}{\omega_2}\right)^2 e_o\left(\frac{1}{2}-e_o\right)\right] + 2\left(\frac{1}{2}+e_o\right)\left(\frac{\omega_1}{\omega_2}\right)^2\left[r_\alpha^2 + 1/8 - e_o\left(\frac{1}{2}-e_o-2x_\alpha\right)\right]}$$

For the case $\omega_1/\omega_2 = 0$, this equation reduces to

$$\mu_{CR} = \frac{1}{\frac{1}{2} + e_o + x_\alpha} \tag{70}$$

which is in agreement with the results presented in two of the earlier studies.[1,2]

Three-Dimensional Lifting Surface Theory

In order to utilize the three-dimensional indicial representation of the hydrodynamic forces, the integral equations (56a), (56e), (57a), and (57b) must be solved numerically, and the three-dimensional indicial hydrodynamic derivatives must be evaluated by means of Equation (59). These integral equations and the corresponding kernel functions were derived and discussed at greater length by Henry.[6] The indicial-response technique is the subject of a subsequent investigation not yet completed, so that numerical results are not available at this time.

It should be noted that the indicial response has a much wider range of application than is used here. When introduced in the equations of motion, the indicial response functions, together with the Duhamel superposition principle, yield expressions for the hydrodynamic forces in terms of the unknown motions.[6] The resulting equations can be used to study a wide variety of problems associated with the transient response of hydrofoil craft. These include: (1) flutter analysis; (2) prediction of mode shapes and natural frequencies in the flying condition (including the effect of forward speed); (3) elastic and rigid body response to free-surface wave excitation, pressure waves from underwater explosions, control deflections, internal vibration sources, etc.; (4) digital or analog hydrofoil-boat simulation; and many others.

EXPERIMENTAL ANALYSIS

The Davidson Laboratory flutter apparatus, which was used in these tests, has been described in the first of these hydroelastic studies.[1] The lower end plate was removed in order to obtain three-dimensional flow. The flexure system described in the second study[2] was used to support the models of the present study (the thickness of the flexures in the rotation flexure beams was reduced to 0.025 in.). The properties of this apparatus, with no weights or models attached, are given in Table 1.

Three models were tested. Two had rectangular planform, with 6-in. chord, 12-in. span and 6-in. chord, 6-in. span, respectively. The third had a 15-degree sweep angle, a taper ratio of 1/3, 6-in. root chord, and 12-in. span normal to the flow direction. The plastic model described in the first investigation of this series[1] was used as the first model, then was cut in half for use as the second one. The third model was machined from aluminum stock by means of an airfoil milling machine. The weights and center-of-gravity locations of the models are given in Table 2.

Two systems of weights were used to obtain the desired values of center-of-gravity location, radius of gyration, and natural-frequency ratio, as described in the first study.[1] Two center-of-gravity weights were used, each weighing 0.5 lb and located as shown in Table 3. The positions were determined to provide the desired value of center-of-gravity location and natural-frequency ratio. Each of the additional cylindrical weights had a radius of 3.285 inches.

The stiffnesses of the translation and rotation flexures per unit span are given in Table 1. With these constants, the density ratio and radius of gyration were determined (just before testing each configuration) from the uncoupled natural frequencies measured in air for translation ω_1 and rotation ω_2, by means of

$$\mu = \frac{K_1}{\omega_1^{2}\pi\rho b_o^{2}}$$

$$r_\alpha^{\,2} = \frac{K_2}{K_1 b_o^{\,2}} \left(\frac{\omega_1}{\omega_2}\right)^2$$

This value of μ was found to be in agreement with that calculated from the known change in mass of the apparatus. The measured frequencies are shown in Table 3, together with the values of μ and $r_\alpha^{\,2}$.

The model was held away from its equilibrium position while the apparatus accelerated, then was released and its resulting motions recorded. Test speed was increased in each subsequent run, until an unstable condition was reached. It was found that when the apparatus was returned at a very low speed, the water in the tank became calm very quickly after each run. No less than five minutes elapsed between runs.

Subsequent to each run, the records were analyzed for the frequency and logarithmic decrement. After completion of the experiments, these calculations were checked, and the reduced speed $U/b\omega_\alpha$, frequency ratio ω/ω_α , and decay rate σ/ω_α were computed. All tests were made close to the expected flutter speed; hence only the lightly damped mode of response appeared in the records. The results are presented in Table 4 and in Figures 2, 3, and 4.

DISCUSSION OF RESULTS

Measured values of decay rate, frequency, and flutter speed are compared herein with corresponding results predicted by two-dimensional airfoil theory applied in a stripwise manner. Using the results of three-dimensional lifting-surface theory, the flutter speed for one hydrofoil model was predicted.

The dynamic configuration studied here is a hydrofoil elastically restrained in translation normal to its plane and in rotation about a spanwise axis normal to the stream direction. Three hydrofoil geometries were considered: two with rectangular planform, with span-chord ratios of 2 and 1; and one with span-chord ratio of 2, midchord sweep angle of 15 degrees, and taper ratio of 1/3. The geometric, elastic, and inertial properties of the tested models are summarized in Tables 2 and 3, while the non-dimensional values of speed, frequency, and decay rate (which were found from the test records) are exhibited in Table 4. The measured decay rate and frequency for Model 1, with rectangular planform and aspect ratio of 4 (the effective hydrodynamic aspect ratio is twice the span-to-chord ratio, due to the presence of the upper end plate, which was retained in these tests), are shown in Figure 2 for the five values of density ratio μ which were tested. The corresponding theoretical results, predicted by the two-dimensional methods described in the third of the earlier studies,[3] are also shown. The predicted frequency is in agreement with measured values at all density ratios. The predicted decay rate is in agreement with measured values at the density ratios 1.86 and 2.96. However, at the intermediate values 2.26, 2.37, and 2.54, the theory predicts values higher than those measured. These observations are in agreement with those of the authors' previous studies.[1,2,3]

The same comparison is made in Figure 3, for Model 2 with rectangular planform and aspect ratio 2. At this aspect ratio, the measured and predicted values of frequency begin to show some discrepancies at the higher speeds $(U/b\omega_\alpha > 2.4)$. Furthermore, the measured and predicted values of decay rate are not in agreement at any values of density ratio. Thus, below aspect ratio 3, the results of the two-dimensional strip theory described in the third study[3] must be considered unreliable.

The measured flutter speeds for Models 1 and 2 are compared in Figure 4 with values predicted by the stripwise, two-dimensional flutter-analysis procedure described previously in this report. In addition, the measured flutter speeds for this configuration in two-dimensional flow, described in the report of the second study,[2] are replotted here in Figure 4. These results show that decreasing aspect ratio results in an increase in non-dimensional flutter speed, while the critical density ratio appears to be unchanged. At aspect ratio 4, the measured two-degree-of-freedom flutter speeds show little aspect-ratio effect for rectangular planforms. This observation should not be extrapolated to ranges of parameters outside those tested here, nor to other planforms and dynamic configurations.

Also shown in Figure 4 is a flutter speed predicted for the Model 1 configuration, based upon the results of three-dimensional lifting-surface theory. The non-conservative tendency found here in the comparison between measured and predicted flutter speed for this three-dimensional configuration is the same as was found for two-dimensional flow in the first two of these studies.[1,2] A considerable number of difficulties were encountered in attempting to find the numerical solution to the double integral equation (37). In fact, many numerical difficulties arise in all the methods of solution applied to this surface integral equation.[5,8,9,10] In particular, it has been found that the numerical scheme for the chordwise integration must be carried out with extreme accuracy[9] and with proper accounting for the large curvature of the integrand near leading and trailing edges, the oscillatory nature of the integrand, and the finite jump occurring in the kernel function.

On the other hand, in an investigation now in progress, it has been found that by introducing the lift-operator approach, as was done in unsteady lifting-surface propeller theory,[11] the following advantages are gained:

(1) The convergence of the series expansion of the induced velocity is improved by the introduction of an additional converging factor.

(2) A desired accuracy of loading can be achieved with fewer loading modes, since the specified downwash distribution is obtained in a weighted-average sense over the whole chord.

(3) By introducing an appropriate expansion of the kernel function, the chordwise integration can be carried out analytically.

As a result of 2 and 3, the computer time required to solve the downwash integral equation is reduced considerably. Thus, further development of the lift-operator technique in the solution of the lifting-surface integral equation is of paramount importance.

A third model with sweep, taper, and finite span was tested in this investigation, at one value of density ratio and with effective hydrodynamic aspect ratio of 6. The flutter speed predicted for this model by means of two-dimensional strip theory is shown in Figure 5, where it is also indicated that no flutter was found at any speed up to 1.5 times the predicted flutter speed. In fact, Table 4 shows that, at reduced speeds above 2.0, no oscillatory response was observed. This conservative discrepancy between measured and predicted flutter speeds is not in agreement with any previous observations. Thus, the application of two-dimensional strip theory to this planform is not valid. Therefore, the results of two-dimensional theory used in a stripwise manner to predict flutter speeds of hydrofoils in three-dimensional flow cannot be considered reliable for planforms with sweep and taper.

CONCLUSIONS AND RECOMMENDATIONS

Measured values of decay rates, frequencies, and flutter speeds of hydrofoils are compared herein for the case of a two-degree-of-freedom system. Three hydrofoil models are considered: two with rectangular planforms and with effective hydrodynamic aspect ratios of 4 and 2, the other with midchord sweep angle of 15 degrees, taper ratio of 1/3, and effective hydrodynamic aspect ratio of 6. The tests with the first two models were conducted over a range of density ratios.

When the measured values of decay rates, frequencies, and flutter speeds of these two-degree-of-freedom models are compared with those predicted by unsteady two-dimensional airfoil theory applied in a stripwise manner, the following conclusions may be drawn:

(1) Below aspect ratio 3, the results of two-dimensional strip theory must be considered unreliable for use in hydroelastic studies of hydrofoils with rectangular planforms in three-dimensional flow.

(2) For hydrofoils with rectangular planforms, decreasing aspect ratio results in an increase in reduced flutter speed, while the critical density ratio appears to be unchanged.

(3) At aspect ratio 4, the measured two-degree-of-freedom flutter speeds show little effect of aspect ratio for the case of rectangular planform.

(4) The results of two-dimensional strip theory cannot be considered reliable in hydroelastic studies of hydrofoils with sweep and taper in three-dimensional flow.

The flutter speed predicted for the rectangular foil with aspect ratio 4, by means of three-dimensional lifting-surface theory, shows, when compared with the corresponding measured values, the same non-conservative tendency found previously for two-dimensional flow.

Due to the many difficulties which arise in the numerical treatment of the double-integral equation of lifting-surface theory, it is recommended that continued effort on the lift-operator technique be considered of paramount importance, since this method seems to have many advantages over other techniques presently used.

REFERENCES

1. HENRY, C. J., "Hydrofoil Flutter Phenomenon and Airfoil Flutter Theory; Vol. I, Density Ratio," DL Report 856, September 1961.

2. HENRY, C. J. and ALI, M. R., "Hydrofoil Flutter Phenomenon and Airfoil Flutter Theory; Vol II, Center of Gravity Location," DL Report 911, July 1962.

3. HENRY, C. J. and ALI, M. R., "Hydrofoil Flutter Phenomenon and Airfoil Flutter Theory; Vol. III, Sweep and Taper," DL Report 1115, December 1965.

4. WATKINS, C. E., WOOLSTON, D. S., CUNNINGHAM, H. J., "A Systematic Kernel Function Procedure for Determining the Aerodynamic Forces on Oscillating or Steady Finite Wings at Subsonic Speeds," NASA TR R-48, 1959.

5. TSAKONAS, S. and HENRY, C. J., "Finite Aspect Ratio Hydrofoil Configurations in a Free Surface Wave System," DL Report 1118, June 1966.

6. HENRY, C. J., "Three-Dimensional Indicial Pressure Loading on Hydrofoils." Dissertation, SIT, June 1965.

7. DRISCHLER, J. A., "An Integral Equation Relating the General Time-Dependent Lift and Downwash Distributions on Finite Wings in Subsonic Flow," NASA TN D-1521, January 1963.

8. WILLIAMS, D. E., Manual on Aeroelasticity, Part II, Aerodynamic Aspects; Chap. 3, "Three-Dimensional Subsonic Theory." W. P. Jones, General Editor; NATA, AGARD.

9. ROWE, W. S., "Collocation Method for Calculating the Aerodynamic Pressure Distributions on a Lifting Surface Oscillating in Subsonic Compressible Flow," AIAA Symposium on Structural Dynamics and Aeroelasticity, September 1965.

10. REVELL, J. D. and RODDEN, W. P., "Remarks on Numerical Solutions of the Unsteady Lifting Surface Problem, " AIAA Journal, Vol. 4, No. 1, January 1966.

11. TSAKONAS, S. and JACOBS, W. R., "Unsteady Lifting Surface Theory for a Marine Propeller of Low Pitch Angle with Chordwise Loading Distribution," DL Report 994, January 1964; J. Ship Research, Vol. 9, No. 2, September 1965.

TABLE 1

PROPERTIES OF DAVIDSON LABORATORY FLUTTER APPARATUS

[With no weights or models; reference span length, 12 in. and reference chord length 6 in.]

$K_h = 0.203$ lb/in.[a]

$K_\alpha = 3.68$ in.-lb/in.-rad

$\omega_{h_o} = 13.28$ rad/sec

$\omega_{\alpha_o} = 48.70$ rad/sec

$\mu_o = 0.413$

$r_{\alpha_o} = 0.1495$

$x_{\alpha_o} = 0.0923$

TABLE 2

PROPERTIES OF MODELS

Model	Description	μ_m	x_{α_m}	e_o
1	Span-chord ratio 2	0.123	0.350	-0.5
2	Span-chord ratio 1	0.061	0.350	-0.5
3	Span-chord ratio 2 Sweep angle 15° Taper ratio 1/3	0.140	0.647	-0.5

TABLE 3

MEASURED PROPERTIES OF TEST CONFIGURATIONS

Model	Position of CG weights (1) (in.)	(2)	x_α	ω_h $\frac{rad}{sec}$	μ	ω_α $\frac{rad}{sec}$	r_α^2	$\frac{\omega_h}{\omega_\alpha}$
1	-3.4	6.2	0.195	6.44	1.86	12.08	0.571	0.533
				5.83	2.26	10.92	0.573	0.534
				5.70	2.37	10.62	0.580	0.537
				5.50	2.54	10.34	0.569	0.532
				5.10	2.96	9.57	0.571	0.533
2	-3.2	5.8	0.167	11.48	1.16	22.93	0.504	0.501
				10.39	1.42	20.43	0.521	0.509
				7.84	2.50	14.89	0.558	0.527
				6.56	3.58	12.30	0.571	0.533
				5.16	5.76	9.70	0.571	0.533
3	-4.9	4.1	0.190	5.08	2.98	9.52	0.573	0.534

TABLE 4

MEASURED RESPONSE CHARACTERISTICS

Model	μ	$U/b\omega_\alpha$	ω/ω_α	$\omega b/U$	σ/ω_α
1	1.86	1.64	0.847	0.517	-0.103
		2.00	0.847	0.424	-0.076
		2.31	0.847	0.367	-0.062
		2.63	0.850	0.323	-0.066
		2.30	0.827	0.360	-0.055
		2.31	0.833	0.361	-0.084
		2.62	0.842	0.322	-0.066
		2.94	0.854	0.280	-0.073
		1.60	0.854	0.534	-0.103
		2.34	0.845	0.361	-0.040
	2.26	2.12	0.848	0.400	-0.022
		2.57	0.845	0.329	+0.011
		2.55	0.840	0.330	-0.005
	2.37	2.30	0.836	0.364	-0.001
		2.70	0.837	0.310	+0.027
		2.24	0.840	0.375	-0.006
	2.54	2.33	0.833	0.358	0
		1.46	0.868	0.595	-0.086
		1.93	0.837	0.434	-0.039
		2.38	0.836	0.351	+0.014
	2.96	1.60	0.863	0.540	-0.093
		1.98	0.836	0.422	-0.040
		2.40	0.845	0.352	+0.017
		2.50	0.832	0.333	+0.022
		2.08	0.836	0.402	-0.017
		2.22	0.832	0.375	+0.011
2	1.42	1.39	0.827	0.595	-0.185
		1.56	0.827	0.530	-0.194
		1.75	0.805	0.460	-0.165
		2.38	0.827	0.348	-0.130
		2.77	0.775	0.280	-0.109

Table 4 (Cont'd)

Model	μ	$U/b\omega_\alpha$	ω/ω_α	$\omega b/U$	σ/ω_α
	2.50	1.90	0.824	0.433	-0.054
		2.39	0.814	0.342	0
		2.74	0.839	0.306	+0.013
		2.56	0.811	0.317	+0.041
		2.18	0.817	0.375	-0.015
	3.58	2.34	0.818	0.350	+0.013
		2.43	0.814	0.335	+0.021
		2.27	0.818	0.360	-0.008
		2.16	0.826	0.383	-0.020
2	5.76	2.05	0.860	0.420	-0.070
		2.50	0.910	0.364	+0.017
		2.26	0.830	0.367	-0.027
3	2.98	1.51	1.16	0.768	-0.270
		1.58	1.20	0.760	-0.389
		2.06	No oscillatory response!		
		2.45			
		2.91			

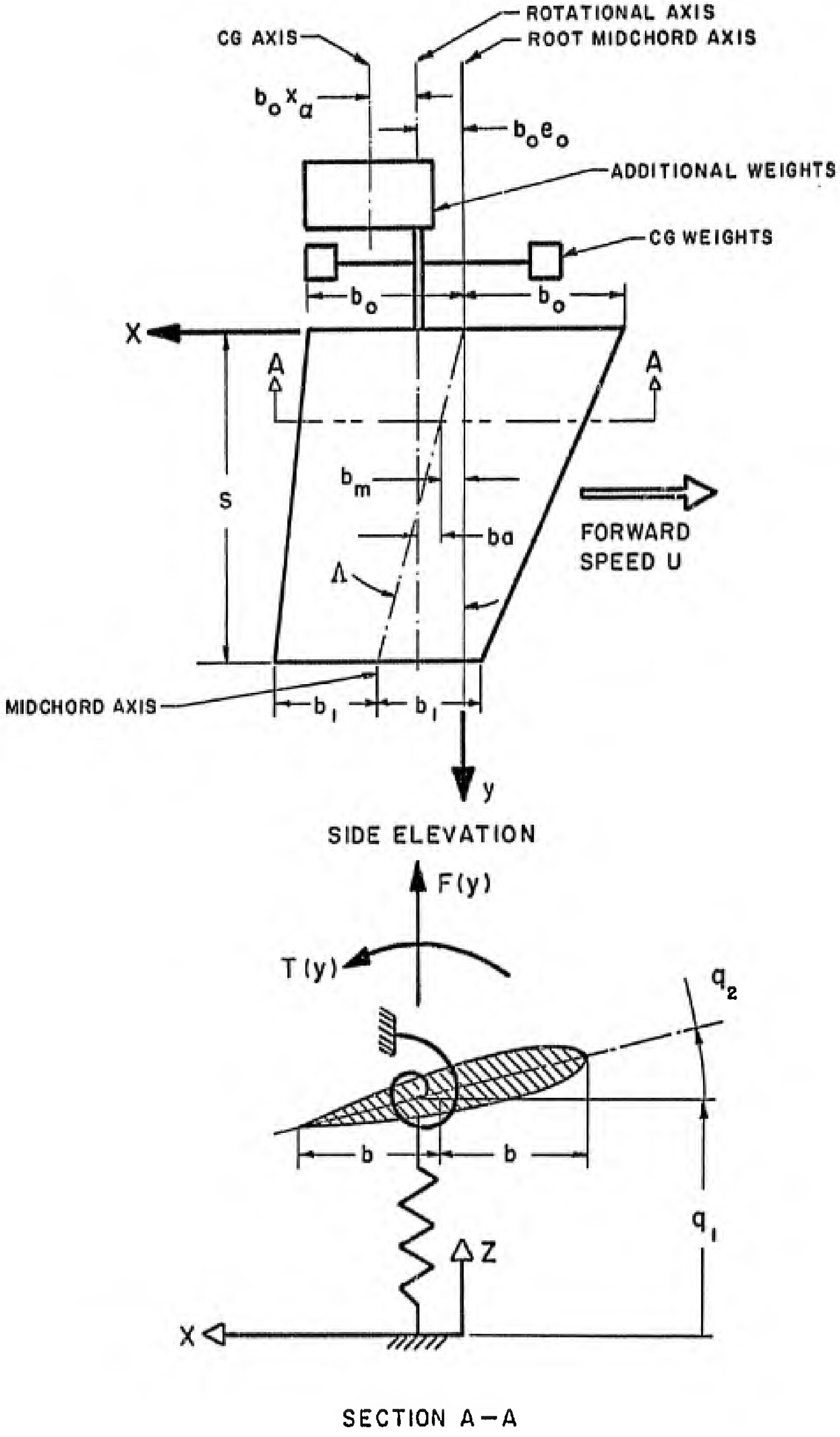

FIGURE 1. SCHEMATIC DIAGRAM OF HYDROFOIL MODEL WITH DEFINITION OF PARAMETERS AND COORDINATE SYSTEM

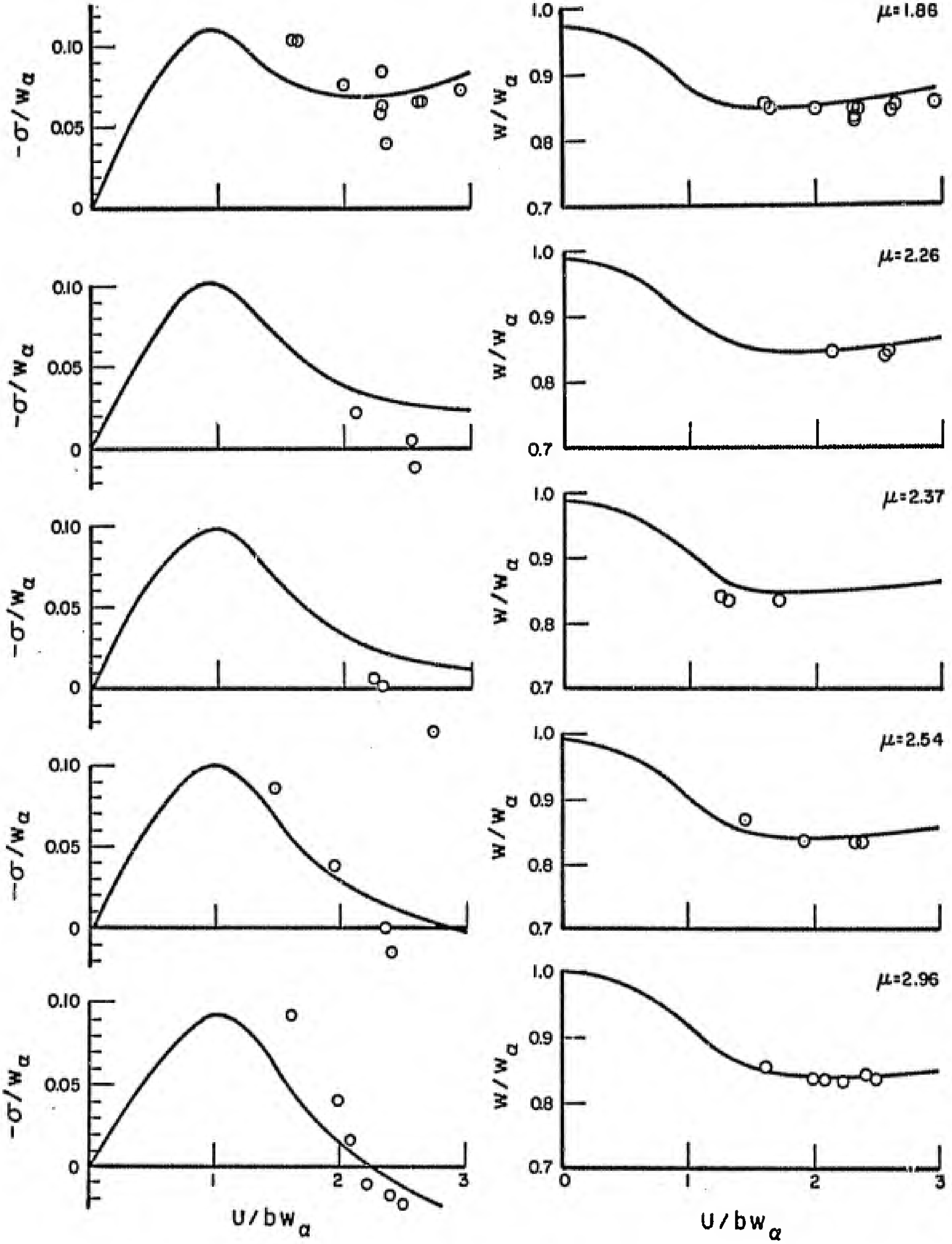

FIGURE 2. RESPONSE CHARACTERISTICS – MODEL I

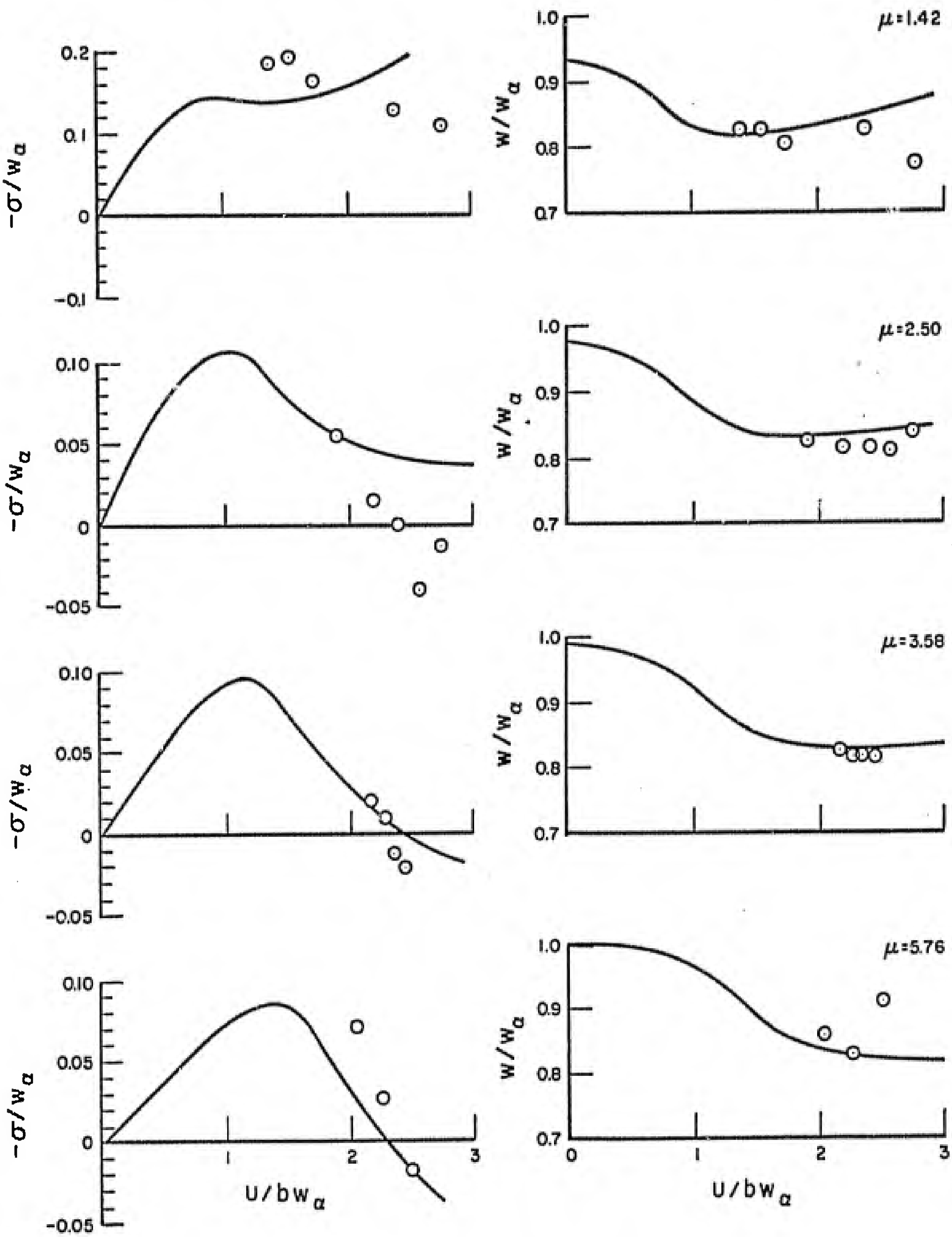

FIGURE 3. RESPONSE CHARACTERISTICS - MODEL 2

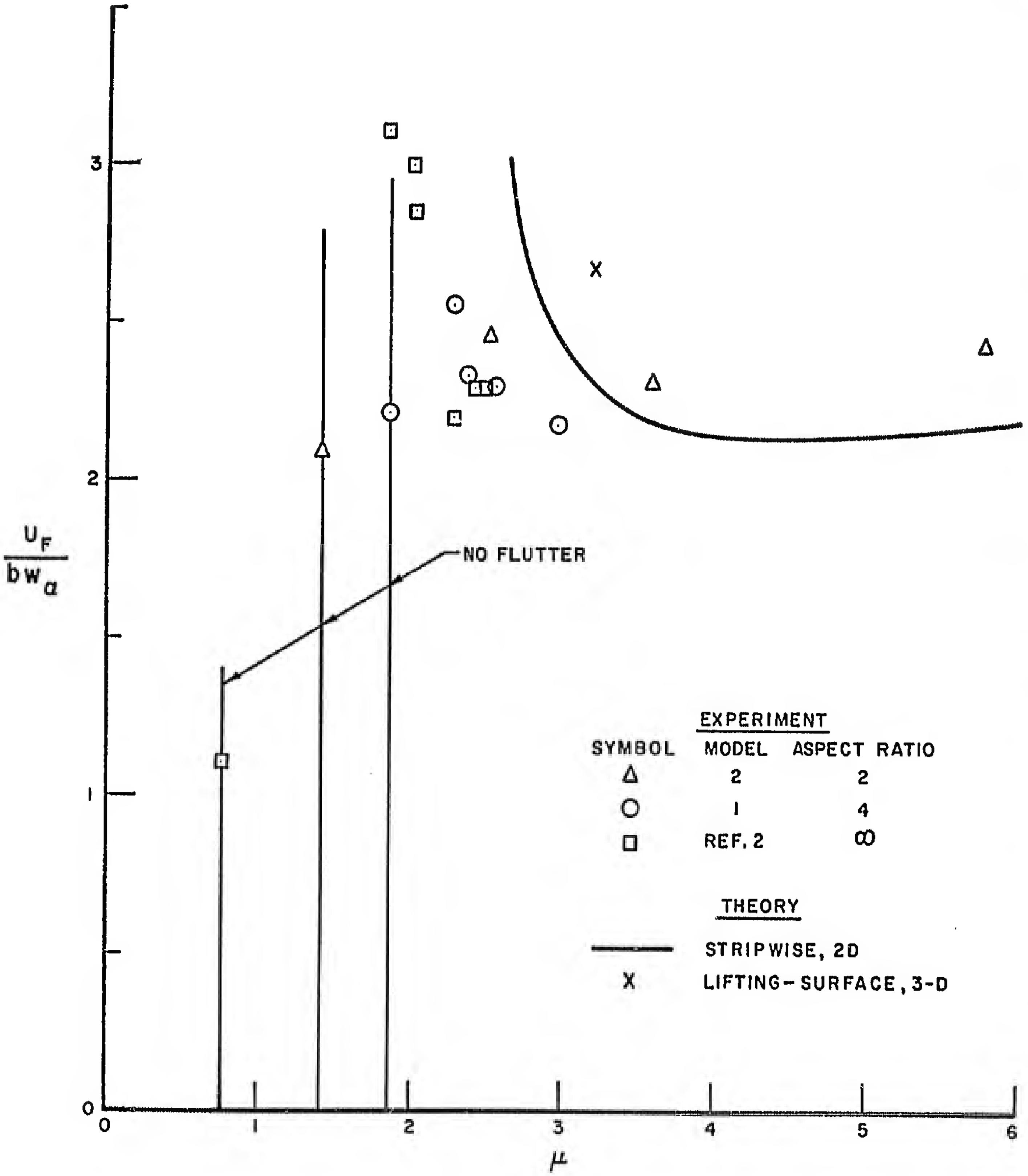

FIGURE 4. EFFECT OF ASPECT RATIO ON FLUTTER SPEED

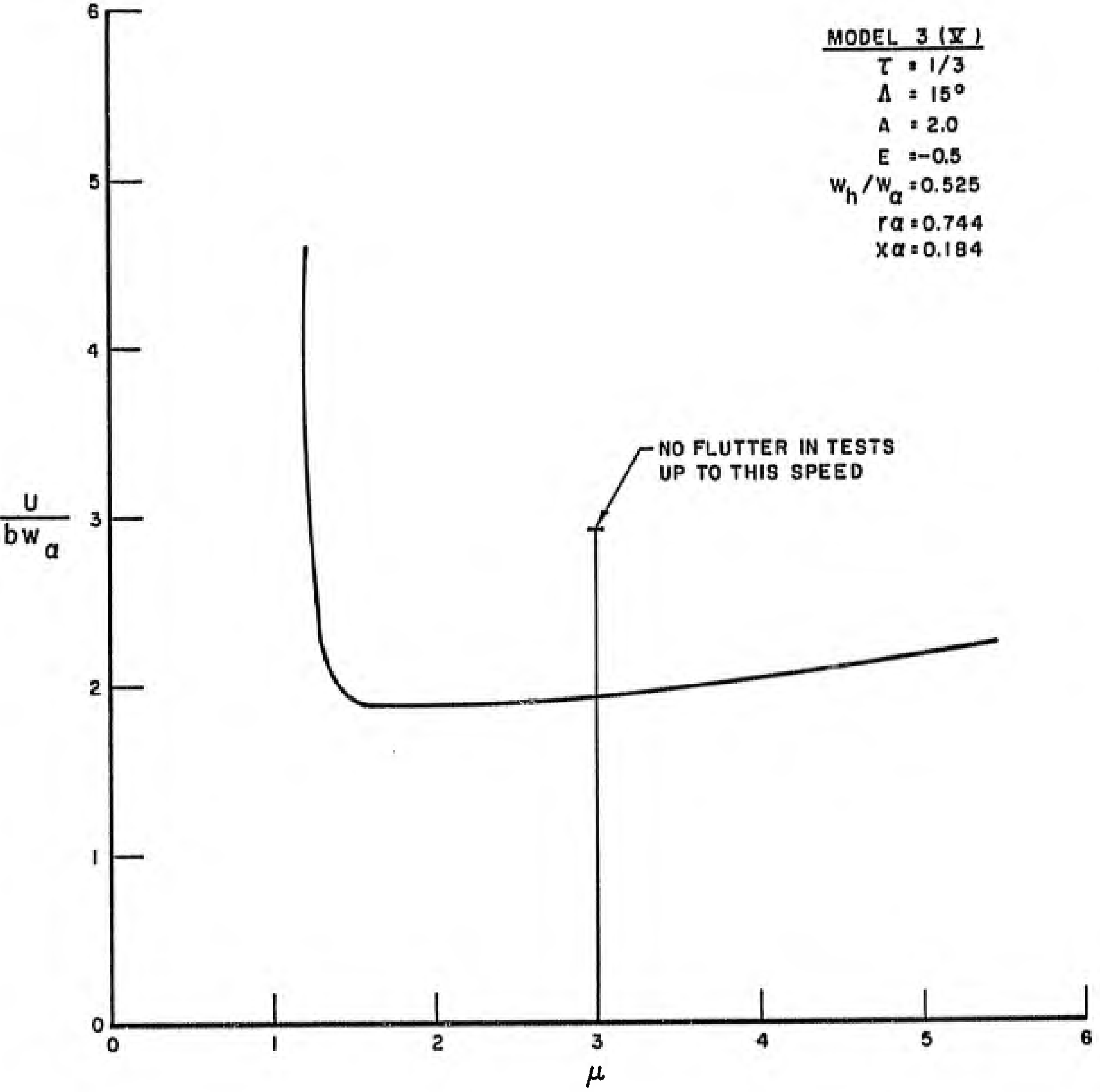

FIGURE 5. EFFECT OF TAPER AND SWEEP ANGLE ON FLUTTER SPEED

UNCLASSIFIED

Security Classification

DOCUMENT CONTROL DATA - R&D

(Security classification of title, body of abstract and indexing annotation must be entered when the overall report is classified)

1. ORIGINATING ACTIVITY (Corporate author) Davidson Laboratory, Stevens Institute of Technology	2a. REPORT SECURITY CLASSIFICATION Unclassified 2b. GROUP

3. REPORT TITLE

HYDROFOIL FLUTTER PHENOMENON AND AIRFOIL FLUTTER THEORY
Volume IV, Finite Aspect Ratio

4. DESCRIPTIVE NOTES (Type of report and inclusive dates)

Final

5. AUTHOR(S) (Last name, first name, initial)

Henry, Charles J.

Ali, M. Raihan

6. REPORT DATE	7a. TOTAL NO. OF PAGES	7b. NO. OF REFS
October 1966	ix + 41	11

8a. CONTRACT OR GRANT NO. NObs 88365	9a. ORIGINATOR'S REPORT NUMBER(S)
b. PROJECT NO. Serial No. SS 600-00 Task 1719	Report 1170
c.	9b. OTHER REPORT NO(S) (Any other numbers that may be assigned this report)
d.	

10. AVAILABILITY/LIMITATION NOTICES

Qualified requesters may obtain copies of this report from DDC.

11. SUPPLEMENTARY NOTES	12. SPONSORING MILITARY ACTIVITY
	Bureau of Ships Department of the Navy

13. ABSTRACT

Measured decay rates and flutter speeds for two-degree-of-freedom hydrofoil models with finite aspect ratio are compared with those predicted by two-dimensional airfoil theory applied in a stripwise manner. The flutter speed of one of the experimental configurations is also predicted by means of three-dimensional lifting-surface theory. Both theory and experiment indicate that flutter speed increases as aspect ratio is decreased. However, the non-conservative discrepancy found previously between measured and predicted two-degree-of-freedom flutter speeds in two-dimensional flow persists in these three-dimensional results.

DD FORM 1 JAN 64 1473

UNCLASSIFIED

Security Classification

14. KEY WORDS	LINK A ROLE	LINK A WT	LINK B ROLE	LINK B WT	LINK C ROLE	LINK C WT
Hydroelasticity						
Flutter						

INSTRUCTIONS

1. ORIGINATING ACTIVITY: Enter the name and address of the contractor, subcontractor, grantee, Department of Defense activity or other organization *(corporate author)* issuing the report.

2a. REPORT SECURITY CLASSIFICATION: Enter the overall security classification of the report. Indicate whether "Restricted Data" is included. Marking is to be in accordance with appropriate security regulations.

2b. GROUP: Automatic downgrading is specified in DoD Directive 5200.10 and Armed Forces Industrial Manual. Enter the group number. Also, when applicable, show that optional markings have been used for Group 3 and Group 4 as authorized.

3. REPORT TITLE: Enter the complete report title in all capital letters. Titles in all cases should be unclassified. If a meaningful title cannot be selected without classification, show title classification in all capitals in parenthesis immediately following the title.

4. DESCRIPTIVE NOTES: If appropriate, enter the type of report, e.g., interim, progress, summary, annual, or final. Give the inclusive dates when a specific reporting period is covered.

5. AUTHOR(S): Enter the name(s) of author(s) as shown on or in the report. Enter last name, first name, middle initial. If military, show rank and branch of service. The name of the principal author is an absolute minimum requirement.

6. REPORT DATE: Enter the date of the report as day, month, year; or month, year. If more than one date appears on the report, use date of publication.

7a. TOTAL NUMBER OF PAGES: The total page count should follow normal pagination procedures, i.e., enter the number of pages containing information.

7b. NUMBER OF REFERENCES: Enter the total number of references cited in the report.

8a. CONTRACT OR GRANT NUMBER: If appropriate, enter the applicable number of the contract or grant under which the report was written.

8b, 8c, & 8d. PROJECT NUMBER: Enter the appropriate military department identification, such as project number, subproject number, system numbers, task number, etc.

9a. ORIGINATOR'S REPORT NUMBER(S): Enter the official report number by which the document will be identified and controlled by the originating activity. This number must be unique to this report.

9b. OTHER REPORT NUMBER(S): If the report has been assigned any other report numbers *(either by the originator or by the sponsor)*, also enter this number(s).

10. AVAILABILITY/LIMITATION NOTICES: Enter any limitations on further dissemination of the report, other than those imposed by security classification, using standard statements such as:

(1) "Qualified requesters may obtain copies of this report from DDC."

(2) "Foreign announcement and dissemination of this report by DDC is not authorized."

(3) "U. S. Government agencies may obtain copies of this report directly from DDC. Other qualified DDC users shall request through
_______________________________."

(4) "U. S. military agencies may obtain copies of this report directly from DDC. Other qualified users shall request through
_______________________________."

(5) "All distribution of this report is controlled. Qualified DDC users shall request through
_______________________________."

If the report has been furnished to the Office of Technical Services, Department of Commerce, for sale to the public, indicate this fact and enter the price, if known.

11. SUPPLEMENTARY NOTES: Use for additional explanatory notes.

12. SPONSORING MILITARY ACTIVITY: Enter the name of the departmental project office or laboratory sponsoring *(paying for)* the research and development. Include address.

13. ABSTRACT: Enter an abstract giving a brief and factual summary of the document indicative of the report, even though it may also appear elsewhere in the body of the technical report. If additional space is required, a continuation sheet shall be attached.

It is highly desirable that the abstract of classified reports be unclassified. Each paragraph of the abstract shall end with an indication of the military security classification of the information in the paragraph, represented as *(TS), (S), (C), or (U)*.

There is no limitation on the length of the abstract. However, the suggested length is from 150 to 225 words.

14. KEY WORDS: Key words are technically meaningful terms or short phrases that characterize a report and may be used as index entries for cataloging the report. Key words must be selected so that no security classification is required. Identifiers, such as equipment model designation, trade name, military project code name, geographic location, may be used as key words but will be followed by an indication of technical context. The assignment of links, roles, and weights is optional.